

# Selective colorimetric sensors for cyanide and acetate ion in partially aqueous medium

Divya Singhal, Neha Gupta, Ashok Kumar Singh\*  
Department of Chemistry, Indian Institute of Technology Roorkee  
Roorkee-247667, India  
\*E-mail: [akscyfcy@iitr.ernet.in](mailto:akscyfcy@iitr.ernet.in)

## Abstract

4-(thiazol-2-yl-diazenyl)phenol ( $L_1$ ) and 2-((4-hydroxyphenyl) diazenyl)-5-nitrophenol ( $L_2$ ) based on azo phenol were synthesised and used as selective colorimetric sensor for  $CN^-$  and  $AcO^-$  ion in DMSO/ $H_2O$ -HEPES (v/v; 1:1, pH-7.3 $\pm$ 0.2) and showed good sensitivity with large red shifts and nanomolar detection limit for  $CN^-$  and  $AcO^-$  ion. The stoichiometry of  $L_1$  with  $CN^-/AcO^-$  ion was found to be 1:1 and  $L_2$  with  $CN^-/AcO^-$  ion was found to be 1:2. Binding constant for  $L_1 + CN^-$ ,  $L_1 + AcO^-$ ,  $L_2 + CN^-$  and  $L_2 + AcO^-$  were calculated by B-H plot as  $1.6 \times 10^3$ ,  $8.0 \times 10^2$ ,  $8.4 \times 10^3$  and  $1.7 \times 10^2$  respectively.  $L_2$  showed high selectivity towards  $CN^-$  ion with low detection limit of 81 nM and large binding constant. In addition,  $^1H$  NMR titration and DFT studies also supported the deprotonation mechanism of receptors in the presence of selective anions.

**Keywords:** Chemosensors,  $CN^-$  selective sensor, Test strip sensor

## 1. Introduction

In supramolecular chemistry, the development of chromogenic sensor is of great interest in anion sensing due to their chemical and biological applications [1]. The most hazardous cyanide ion widely used in the various chemical industries (140,000 tons of cyanide per year) causes the severe pollution of water supplies [2-3]. Cyanide is extremely toxic, increases environmental pollution due to its industrial use mainly production of textiles, papers and plastics. Importantly, cyanide rigorously suppresses the transport of oxygen as it binds with cytochrome c oxidase and effects electron transfer from cytochrome c oxidase to oxygen in mitochondria [4]. Acetate ion is more important in living organisms as acetyl coenzyme [5].

There are many conventional detection methods for quantitative determination of cyanide and acetate ion mainly based on electrochemical and voltammetric techniques [6-10]. Due to their cost and sophisticated instruments, detection of cyanide and acetate ion by absorption or fluorescence or both studies are easier and growing very fast [11-15]. So the development of colorimetric anion sensor is more attractive due to no requirement of expensive equipment as color changes can be easily detected by the naked-eye. Generally, the chromogenic anion sensor consisted many pathways as: displacement of a metal complex (Fig. 1), anion receptor and chromophore, these sensors having chromogenic centre that is covalently bonded to the receptor unit. The receptor unit or binding sites are based on hydrogen bond donor group, generally –OH and –NH group of phenols, sulphonamide, urea, thiourea [16-19]. Compared to the above traditional chemosensor method, an alternative chemodosimeter approach based on an irreversible specific chemical reaction has emerged as an active research area of significant importance. However, considerable efforts have been devoted to the development of a chemodosimeter for anions. Many examples are available about colorimetric sensors for acetate and cyanide ion in the literatures [20-28].

In this paper, we described two phenol based azo dyes  $L_1$  and  $L_2$  which selectively sense biologically important  $CN^-$  and  $AcO^-$  ion in partially aqueous medium without any interference of different anions. Two azo dye based ligands were synthesised having phenolic group for better sensing ability towards anions, resulting in the enhancement of push-pull approach of intramolecular charge transfer (ICT), which reproduced red-shifted absorption. Azo dye ligand  $L_2$  with  $-NO_2$  units (electron-withdrawing substituent) performed high selective binding ability towards cyanide ion over other studied ion.

## 2. Experimental Section

### 2.1. Reagents and Instruments

Analytical grade anion salts are purchased from Merck. Phenol, 2-aminothiazole and 2-amino-5-nitrophenol were purchased from Sigma-Aldrich. CHNS analysis was recorded on an Elementar model Vario EL-III. IR spectra were obtained using a Perkin Elmer FT-IR 1000 spectrophotometer as films between KBr.  $^1\text{H}$  NMR spectra were recorded on Bruker AVANCE 500 MHz spectrometer and Zeol 400 MHz spectrometer. UV-vis spectra were recorded on Shimadzu, UV-3600 double beam spectrophotometer using 10 mm path length of silica cell. DFT computational studies were obtained with Gaussian 09 W programme in gas phase using a B3LYP function with 6-31G(d,p) basis set for  $\text{L}_1$ ,  $\text{L}_2$ ,  $\text{L}_1+\text{CN}^-$  and  $\text{L}_2+\text{CN}^-$ .

### 2.2. Results and Discussion

#### 2.2.1. Synthesis of Azo dyes:

##### Synthesis of 4-(thiazol-2-yl-diazenyl)phenol ( $\text{L}_1$ )

4-(thiazol-2-yl-diazenyl)phenol ( $\text{L}_1$ ) was synthesised based on the previously reported literature [29]. 1 gm of 2-aminothiazole was dissolved in 12 ml of  $\text{H}_2\text{SO}_4$  and then add 0.3 gm of sodium nitrite ( $\text{NaNO}_2$ ) in 10 ml water in dropwise manner with continuous stirring. The mixture was stirred for half an hour at  $0^\circ\text{C}$  (Solution 1). For the coupling reaction, the mixture of 0.9 gm of phenol and 10 ml of 0.1 M NaOH were taken in a separate flask and maintain the temperature at  $0^\circ\text{C}$  (Solution 2). Solution 2 was added in solution 1 while stirring at  $0^\circ\text{C}$ . The formed precipitate washed with distilled water and recrystallised using ethanol and collect the orange powdered product (Scheme 1).

Yield-60 %;  $\text{C}_9\text{H}_7\text{N}_3\text{OS}$ ; C, 52.67; H, 3.44; N, 20.47; O, 7.80; S, 15.62; found C, 52.26; H, 3.4; N, 20.40; O, 8.0; S, 15.94; FTIR (KBr,  $\nu_{\text{max}}$ ,  $\text{cm}^{-1}$ ) –OH: 3436, -N-N, 1591, C-O: 1242, Ar-H: 1143,  $^1\text{H}$  NMR (500 MHz,  $\text{DMSO}-d_6$ , ppm);  $\delta$  10.796 (s, 1H), 8.046 (d, 1H), 7.862 (d, 2H), 7.818 (d, 1H), 6.983 (d, 2H),  $^{13}\text{C}$  NMR (100 MHz,  $\text{DMSO}-d_6$ ): 117.1, 122.3, 126.7, 131.0, 131.6, 144.1, 144.8, 163.4, 177.2 ppm; UV-vis ( $\text{DMSO}$ ,  $\lambda_{\text{max}}$ , nm); 253, 393. [ESI Fig.1 – ESI Fig.7]

##### 2-((4-hydroxyphenyl)diazenyl)-5-nitrophenol ( $\text{L}_2$ )

Took, 2 gm of 2-amino-5-nitrophenol and dissolved in 24 ml of  $\text{H}_2\text{SO}_4$  and then add 0.6 gm of sodium nitrite ( $\text{NaNO}_2$ ) in 10 ml water in dropwise manner on continuous stirring. The mixture was stirred for half hour at  $0^\circ\text{C}$  (Solution 1). For the coupling reaction, the mixture of

1.8 gm of phenol and 10 ml of 0.2 M NaOH were taken in a separate flask and maintain the temperature of this solution at 0°C (Solution 2). Solution 2 was added slowly on stirring at 0°C to the solution 1. The occurred precipitate washed with distilled water and recrystallised by ethanol and collect yellow-orange powder (Scheme 1).

Yield-51 %; C<sub>12</sub>H<sub>9</sub>N<sub>3</sub>O<sub>4</sub>; C, 55.60; H, 3.50; N, 16.21; O, 24.69; found C, 56.30; H, 3.47; N, 16.27.40; O, 23.96; FTIR (KBr,  $\nu_{\max}$ , cm<sup>-1</sup>) –OH; 3429, -N-N; 1585, 1401, Ar-H; 1186; <sup>1</sup>H NMR (500 MHz, DMSO-*d*<sub>6</sub>, ppm);  $\delta$  10.884 (s, 1H), 8.973 (s, 1H), 7.445 (m, 2H), 7.051 (d, 1H), 6.988 (s, 1H), 6.883 (d,1H), 6.688 (d, 2H); <sup>13</sup>C NMR (100 MHz, DMSO-*d*<sub>6</sub>, ppm) 120.6, 121.9, 122.6, 127.0, 128.9, 129.6, 130.1, 132.1, 141.3, 143.3, 165.3, 172.4; UV-vis (DMSO,  $\lambda_{\max}$ , nm); 213, 262, 374.[ESI Fig.1 – ESI Fig.7]

### 2.2.2. Naked Eye Experiments:

The recognition and chromogenic sensing ability of azo dye L<sub>1</sub> and L<sub>2</sub> (20  $\mu$ M) were checked with the sodium salt of a series of anions F<sup>-</sup>, Cl<sup>-</sup>, Br<sup>-</sup>, CN<sup>-</sup>, H<sub>2</sub>PO<sub>4</sub><sup>-</sup>, HPO<sub>4</sub><sup>2-</sup>, SO<sub>4</sub><sup>2-</sup>, SO<sub>3</sub><sup>2-</sup>, AcO<sup>-</sup>, N<sub>3</sub><sup>-</sup> and SCN<sup>-</sup> (200  $\mu$ M) in DMSO/H<sub>2</sub>O-HEPES (v/v; 1:1, pH = 7.3 $\pm$ 0.2) solution. By examine the chromogenic properties of azo dyes L<sub>1</sub> and L<sub>2</sub>, it was found that both ligands showed instant color changes from yellow to violet with more basic anion, CN<sup>-</sup>/AcO<sup>-</sup> and other anions showed no such color changes (Fig. 2). Basicity of anions is known to be in order of CN<sup>-</sup> > AcO<sup>-</sup> > N<sub>3</sub><sup>-</sup> > F<sup>-</sup> > H<sub>2</sub>PO<sub>4</sub><sup>-</sup> > Cl<sup>-</sup> > Br<sup>-</sup> > I<sup>-</sup> [30] and the ability to form hydrogen bond in order of F<sup>-</sup> > AcO<sup>-</sup> > H<sub>2</sub>PO<sub>4</sub><sup>-</sup> > N<sub>3</sub><sup>-</sup> > CN<sup>-</sup> so that both anions with more basic and least H-bonding character might deprotonate the phenolic hydrogen rather than forming H-bonding. Further the sensitivity of azo dyes with CN<sup>-</sup> and AcO<sup>-</sup> ion was analysed by absorption spectra.

### 2.2.3. UV-Vis Analysis:

Upon addition of different anion like F<sup>-</sup>, Cl<sup>-</sup>, Br<sup>-</sup>, AcO<sup>-</sup>, HPO<sub>4</sub><sup>2-</sup>, H<sub>2</sub>PO<sub>4</sub><sup>-</sup>, CN<sup>-</sup> and N<sub>3</sub><sup>-</sup> (200  $\mu$ M), changes in UV-vis absorption spectra of L<sub>1</sub> and L<sub>2</sub> (20  $\mu$ M) with CN<sup>-</sup>/AcO<sup>-</sup> ions were found. Azo dye L<sub>1</sub> exhibited two absorption peak at 253 ( $\pi$ - $\pi^*$  transition), 393 nm (n- $\pi^*$  transition) and L<sub>2</sub> exhibited three absorption peak at 213 ( $\sigma$ - $\sigma^*$  transition), 262 ( $\pi$ - $\pi^*$  transition) and 374 nm (n- $\pi^*$  transition). L<sub>1</sub> showed new absorption band with CN<sup>-</sup> and AcO<sup>-</sup> ion at 486 and 483 nm respectively hence L<sub>2</sub> also showed same behaviour with CN<sup>-</sup> and AcO<sup>-</sup> ion and found a new absorption band at 435 and 437 nm respectively. With this absorption studies, it was confirmed that both azo dye ligands selectively detect cyanide and acetate ion. This new absorption band may occur because of the abstraction of proton with cyanide and acetate ion. The titrations of L<sub>1</sub> (20  $\mu$ M) were performed in DMSO/H<sub>2</sub>O-HEPES (v/v; 1:1,

pH = 7.3±0.2) solution with CN<sup>-</sup> and AcO<sup>-</sup> ion. For the titration, a series of spectra were taken and started by adding the little amount of the anion solution with the help of microsyringe in the quartz cuvettes containing the solution of azo dye (Fig. 3a-3b). The series of UV-vis spectra were taken after each addition and absorbance values were recorded. L<sub>1</sub> exhibits changes in absorption spectra upon addition of CN<sup>-</sup> ion, the band at 393 nm were quenched with consequently increases in the absorption band at 486 nm due to interaction of CN<sup>-</sup> ion with ligand. Titration experiments for L<sub>2</sub> with CN<sup>-</sup> and AcO<sup>-</sup> ion was performed in the same way (Fig. 4a-4b). The absorption spectra of L<sub>2</sub> shown the changes upon addition of CN<sup>-</sup> ion, the band at 374 nm were quenched with consequently increases in absorbance at 435 nm due to interaction of CN<sup>-</sup> ion with ligand. Three isosbestic point were found and showed that free azo dye and adduct (dye + anion) was in equilibrium (L<sub>1</sub>+CN<sup>-</sup>; 417, 301, 258; L<sub>1</sub>+AcO<sup>-</sup>; 433, 298, 267; L<sub>2</sub>+CN<sup>-</sup>; 400, 300, 270; L<sub>2</sub>+AcO<sup>-</sup>; 399, 301, 273). The binding constant of CN<sup>-</sup> and AcO<sup>-</sup> ion with L<sub>1</sub> and L<sub>2</sub> was calculated using BH-plot (Inset; Fig. 3 and 4) and found to be  $1.6 \times 10^3$ ,  $8.0 \times 10^2$ ,  $8.4 \times 10^3$ , and  $1.7 \times 10^2$  respectively. The most important parameter of chemosensor, limit of detection, for cyanide and acetate ion by using L<sub>1</sub> and L<sub>2</sub> were also determined from absorption titrations based on reported procedure [31-32]. The obtained results from absorption titrations were normalised between maximum and minimum absorbance intensities. A plot of  $(A - A_{\min}) / (A_{\max} - A_{\min})$  vs log A<sup>-</sup> (A= CN<sup>-</sup>, AcO<sup>-</sup>) in DMSO-H<sub>2</sub>O (1:1, v/v) gave a linear curve and the point at which linear line crossed to x-axis was familiar to detection limit (ESI Fig. 8). Table 1 lists the detection limit of CN<sup>-</sup> and AcO<sup>-</sup> ions presented by L<sub>1</sub> and L<sub>2</sub>. The detection limit in DMSO-H<sub>2</sub>O (1:1, v/v) was determined to be 87 nM (L<sub>1</sub> + CN<sup>-</sup>), 83 nM (L<sub>1</sub>+ AcO<sup>-</sup>), 81 nM (L<sub>2</sub> + CN<sup>-</sup>), 89 nM (L<sub>2</sub>+ AcO<sup>-</sup>) respectively. 1:1 stoichiometry of the formation of adducts between anion (CN<sup>-</sup> and AcO<sup>-</sup>) and azo dye L<sub>1</sub>. 1:2 stoichiometry between anions (CN<sup>-</sup> and AcO<sup>-</sup>) and azo dye L<sub>2</sub> was found by Job's plot analysis. A plot was obtained by recording the absorbance of equimolar solution (50 μM in DMSO/H<sub>2</sub>O, 1:1, v/v solution) of azo dyes and anion with different mole fraction which show 1:1 stoichiometry of L<sub>1</sub>+CN<sup>-</sup>, L<sub>1</sub>+AcO<sup>-</sup>, L<sub>2</sub>+CN<sup>-</sup> and L<sub>2</sub>+AcO<sup>-</sup> (ESI Fig. 9-10).

#### **2.2.4. Intereference study on sensor performance:**

As we use the both azo dyes for the detection of cyanide and acetate ion, we also tested the absorption response of L<sub>1</sub> and L<sub>2</sub> towards various anions (N<sub>3</sub><sup>-</sup>, HPO<sub>4</sub><sup>2-</sup>, H<sub>2</sub>PO<sub>4</sub><sup>-</sup>, SCN<sup>-</sup>, AsO<sub>2</sub><sup>-</sup>, Cl<sup>-</sup>, Br<sup>-</sup>, SO<sub>4</sub><sup>2-</sup>, SO<sub>3</sub><sup>2-</sup>, NO<sub>2</sub><sup>-</sup>, NO<sub>3</sub><sup>-</sup> and F<sup>-</sup>) and we found that there was no significant changes in the absorption spectra in the presence of various anions under the same conditions. L<sub>1</sub> and L<sub>2</sub> were found to be more selective towards cyanide and acetate ion even in presence of

various other anions (Fig. 5). We have done competitive experiments [33] in the presence of detecting anion (100  $\mu\text{M}$ ) and other anions (100  $\mu\text{M}$ ) with azo dyes (20  $\mu\text{M}$ ) and we found that the absorption spectra of azo dyes with detecting anions remained unaffected with the addition of other anions. This demonstrated that both azo dyes could be used to quantitative detection of cyanide and acetate ion concentration with great selectivity. In the figure 5-a and 5-b, the blue bar indicates the absorption intensity of  $\text{CN}^-$  with azo dye  $\text{L}_1$  and  $\text{L}_2$  and the red bar indicates the absorption intensity of azo dyes with  $\text{CN}^-$  ion in the presence of interfering ions.

### 2.2.5. $^1\text{H-NMR}$ titration:

To know the mechanism of interaction between azo dye and cyanide ion,  $^1\text{H}$  NMR spectra of  $\text{L}_1$  and  $\text{L}_2$  were recorded in absence and presence of cyanide ion.  $\text{L}_1$  shows NMR peak at  $\delta$  10.796 ppm for  $-\text{OH}$  proton and azo dye  $\text{L}_2$  shows NMR peak at 10.884 ppm and 8.973 ppm for hydroxy protons and the rest peak of NMR assigned for aromatic region. After adding  $\text{CN}^-$  ion solution to  $\text{L}_1$  and  $\text{L}_2$ , shake the solution for a while and  $^1\text{H}$  NMR at room temperature were taken which showed all the peaks of NMR were shifted to the upfield region in both azo dye due to the abstraction of phenolic proton or formation of phenolate ion which increased the electronegativity on  $\pi$ - $e^-$  cloud of aromatic region. The peak of  $-\text{OH}$  proton of (10.796 ppm)  $\text{L}_1$  and (10.884 and 8.973 ppm)  $\text{L}_2$  was found to be completely disappeared and aromatic proton signals of  $\text{L}_1$  and  $\text{L}_2$  slightly shifted to upfield region ( $\Delta\delta = 0.1$  ppm and 0.08 ppm respectively). When adding more amount of  $\text{CN}^-$  ion solution, aromatic protons of  $\text{L}_1$  and  $\text{L}_2$  were dramatically shifted into a high field region ( $\Delta\delta = 0.2$  ppm and 0.17 ppm) due to the possible phenolate ion formation. The  $^1\text{H}$  NMR studies, clearly illustrated that the both  $\text{L}_1$  and  $\text{L}_2$  were interacted cyanide ion *via*. deprotonation of  $-\text{OH}$  group (Fig. 6 and 7). From the careful analysis of  $^1\text{H}$  NMR spectra, the colorimetric change could take place partly through proton abstraction. We reasoned that the basic cyanide anions ( $\text{pK}_a < 9.4$ ) are expected to readily abstract the acidic proton of OH group ( $\text{pK}_a < 4$ ).

### 2.2.6. Theoretical Calculations:

To understand the recognition behaviour of phenol based azo dyes  $\text{L}_1$  and  $\text{L}_2$  with cyanide ion, theoretical studies have been done. The optimized geometry of  $\text{L}_1$ ,  $\text{L}_2$ ,  $\text{L}_1 + \text{CN}^-$  and  $\text{L}_2 + \text{CN}^-$  was obtained in gas phase on Gaussian 09 W computational program [34]. HOMO (Highest Occupied Molecular Orbital) and LUMO (Lowest Unoccupied Molecular Orbital) of  $\text{L}_1$ ,  $\text{L}_2$ ,  $\text{L}_1 + \text{CN}^-$  and  $\text{L}_2 + \text{CN}^-$  obtained by optimised geometry and found that the free ligands  $\text{L}_1$  and  $\text{L}_2$  have higher energy gap ( $\Delta E = 2.362$  and 2.236 eV respectively) between

HOMO and LUMO then the adduct  $L_1+CN^-$  and  $L_2+CN^-$  ( $\Delta E = 1.865$  and  $1.773$  eV respectively, Table 2). These computational calculations were performed using Gaussian 09 with B3LYP/6-31G (d,p) basis set. The deprotonation of OH proton of  $L_1$  and  $L_2$  concludes the decrease in energy gap of  $L_1+CN^-$  and  $L_2+CN^-$ . The theoretical calculation leads to the success of experimental results. Fig. 8 shows the optimized structure and Fig. 9 shows HOMO-LUMO energy level diagram of  $L_1$ ,  $L_2$  and their cyanide adduct.

### **2.2.7. Measurement of Anions with Test strips:**

The test strips were prepared by immersing the whatman filter paper in DMSO solution of azo dye  $L_1$  and  $L_2$ . The paper strips were subsequently dried in air to figure out the “dip-stick” method suitability for the detection of both anions [35]. The coated test strips were further immersed in the aqueous solution of  $CN^-$  and  $AcO^-$  ion solution of different concentration and suddenly a fast color change was found from light yellow to violet red (Fig. 10). The development of such a “dip-stick” approach is extremely attractive for “in-the-field” measurements as it does not require any additional equipment.

### **2.2.8. Fast Response**

To know the fast response time of chemosensor  $L_1$  and  $L_2$  towards cyanide ion, changes in absorption spectra was monitored with time. In this sensor, detection of  $CN^-$  ion with  $L_1$  and  $L_2$  was found to be very fast. New absorption band of  $L_1$  and  $L_2$  with  $CN^-$  ion was found at the higher intensity (plateau region) within 10 s and remains stable for 8-11 min. A curve between time v/s ratiometric absorption intensity reveals that reaction was completed in 10 s (Fig. 11).

### **2.2.9. Analytical Application**

To know the applicability of the sensor  $L_1$  and  $L_2$ , it was further used for the quantitative determination of cyanide ion in drinking water. The sample of drinking water was prepared by adding a known amount of cyanide ion ( $2 \mu M$ ). The experiments were performed using absorption spectra of 2 ml volume of sensor sample after adding a known concentration of cyanide ion which found within the linear calibration range. The experiment was repeated three times and the average concentration of cyanide ion in drinking water was found to be  $1.9 \mu M$ . Then, the recovery percentage performed well with relative standard deviation lower than 2%.

### 3. Conclusion

Highly selective chromogenic azo dyes L<sub>1</sub> and L<sub>2</sub> was designed that can detect both CN<sup>-</sup> and AcO<sup>-</sup> ion in 50% aqueous medium via proton abstraction. The stoichiometry of L<sub>1</sub> and L<sub>2</sub> with CN<sup>-</sup>/AcO<sup>-</sup> ion was confirmed in account of Job's plot. *i.e.* 1:1 and 1:2 respectively. The more basic cyanide and acetate ion abstract the more acidic proton of the molecule and allow the formation of phenolate ion. Thus the accumulation of the negative charge on the whole molecule exhibited a large significant red shift in CT band and major changes in color. LOD for CN<sup>-</sup> ion with L<sub>1</sub> and L<sub>2</sub> was found to be 87 and 81 nM and for AcO<sup>-</sup> ion with L<sub>1</sub> and L<sub>2</sub> was found to be 83 and 89 nM respectively. Therefore, the system used to detect the WHO suggested maximum allowed cyanide concentration in drinking water (1.9 mM).

### Acknowledgement

Ms. Divya Singhal is highly thankful to CSIR New Delhi for financial support to undertake this work.

**References:**

1. M. Inouye, 6-Functional dyes for molecular recognition: chromogenic and fluorescent receptors, *Color. Non-Text. Appl.* (2000) 238–274.
2. H. Hachiya, S. Ito, Y. Fushinuki, T. Masadome, Y. Asano and T. Imato, Continuous monitoring for cyanide in waste water with a galvanic hydrogen cyanide sensor using a purge system, *Talanta* 48 (1999) 997–1004.
3. R. Koenig, Wildlife deaths are a grim wake-up call in Eastern Europe, *Science* 287 (2000) 1737-1738.
4. K. W. Kulig, Cyanide Toxicity, U.S. Department of Health and Human Services, Atlanta, GA (1991).
5. Y. H. Qiao, H. Lin, J. Shao and H. K. Lin, A highly selective naked-eye colorimetric sensor for acetate ion based on 1,10-phenanthroline-2,9-dicarboxyaldehyde-di-(p-substitutedphenyl-hydrazone), *Spectrochim. Acta Part A* 72 (2009) 378–381.
6. V. K. Rao, S. R. Suresh, N. B. S. N. Rao and P. Rajaram, An electrochemical sensor for detection of hydrogen cyanide gas, *Bull. Electrochem.* 13 (1997) 327–329.
7. T. Suzuki, A. Hiolki and M. Kurahashi, Development of a method for estimating an accurate equivalence point in nickel titration of cyanide ions, *Anal. Chim. Acta* 476 (2003) 159–165.
8. D. Shan, C. Mousty and S. Cosnier, Subnanomolar cyanide detection at polyphenol oxidase/clay Biosensors, *Anal. Chem.* 76 (2004) 178–183.
9. T. T. Christison and J. S. Rohrer, Direct determination of free cyanide in drinking water by ion chromatography with pulsed amperometric detection, *J. Chromatogr., A* 1155 (2007) 31–39.
10. A. Safavi, N. Maleki and H. R. Shahbaazi, Indirect determination of cyanide ion and hydrogen cyanide by adsorptive stripping voltammetry at a mercury electrode, *Anal. Chim. Acta* 503 (2014) 213–221.
11. M. Dong, Y. Peng, Y. Dong, N. Tang and Y. Wang, A selective, colorimetric, and fluorescent chemodosimeter for relay recognition of fluoride and cyanide anions based on 1,1'-binaphthyl scaffold, *Org. Lett.* 14 (2012) 130–133.
12. F. Wang, L. Wang, X. Chen and J. Yoon, Recent progress in the development of fluorometric and colorimetric chemosensors for detection of cyanide ions, *Chem. Soc. Rev.* 43 (2014) 4312–4324.

13. Y. Sun, Y. Liu, M. Chen and W. Guo, A novel fluorescent and chromogenic probe for cyanide detection in water based on the nucleophilic addition of cyanide to imine group, *Talanta* 80 (2009) 996–1000.
14. S. Y. Na and H. J. Kim, Azo dye-based colorimetric chemodosimeter for the rapid and selective sensing of cyanide in aqueous solvent, *Tetrahedron Lett.* 56 (2015) 493–495.
15. Y. J. Na, G. J. Park, H. Y. Jo, S. A. Lee and C. Kim, A colorimetric chemosensor based on a Schiff base for highly selective sensing of cyanide in aqueous solution: the influence of solvents, *New J. Chem.* 38 (2014) 5769–5776.
16. J. Shao, H. Lin, X. F. Shang, H. M. Chen and H. K. Lin, A novel neutral receptor for selective recognition of  $\text{H}_2\text{PO}_4^-$ , *J. Incl. Phenom. Macrocycl. Chem.* 59 (2007) 371–375.
17. L. Fabbrizzi, M. Licchelli, G. Rabaioli and A. Taglietti, The design of luminescent sensors for anions and ionisable analytes, *Coord. Chem. Rev.* 205 (2000) 85–108.
18. J. Shao, H. Lin, M. Yu, Z. Cai and H. K. Lin, Study on acetate ion recognition and sensing in aqueous media using a novel and simple colorimetric sensor and its analytical application, *Talanta* 75 (2008) 551–555.
19. J. Shao, H. Lin and H. K. Lin, A simple and efficient colorimetric anion receptor for  $\text{H}_2\text{PO}_4^-$ , *Spectrochim. Acta Part A* 70 (2008) 682–685.
20. S. Nishizawa, H. Kaneda, T. Uchida and N. Teramae, Anion sensing by a donor–spacer–acceptor system: an intra-molecular exciplex emission enhanced by hydrogen bond-mediated complexation, *J. Chem. Soc., Perkin Trans. 2* (1998) 2325–2327.
21. R. Kato, S. Nishizawa, T. Hayashita and N. Teramae, A thiourea-based chromoionophore for selective binding and sensing of acetate, *Tetrahedron Lett.* 42 (2001) 5053–5056.
22. G. R. Youa, G. J. Park, S. A. Lee, Y. W. Choi, Y. S. Kim, J. J. Lee and C. Kim, A single chemosensor for multiple target anions: The simultaneous detection of  $\text{CN}^-$  and  $\text{OAc}^-$  in aqueous media, *Sens. Actuators B* 202 (2014) 645–655.
23. D. Udhayakumari, S. Velmathi and M. S. Boobalan, Novel chemosensor for multiple target anions: The detection of  $\text{F}^-$  and  $\text{CN}^-$  ion via different approach, *J. Fluorine Chem.* 175 (2015) 180–184.
24. Y. Sun, G. Wang and W. Guo, Colorimetric detection of cyanide with N-nitrophenyl benzamide derivatives, *Tetrahedron* 65 (2009) 3480–3485.
25. Y. Ding, T. Li, W. Zhu and Y. Xie, Highly selective colorimetric sensing of cyanide based on formation of dipyrin adducts, *Org. Biomol. Chem.* 10 (2012) 4201–4207.

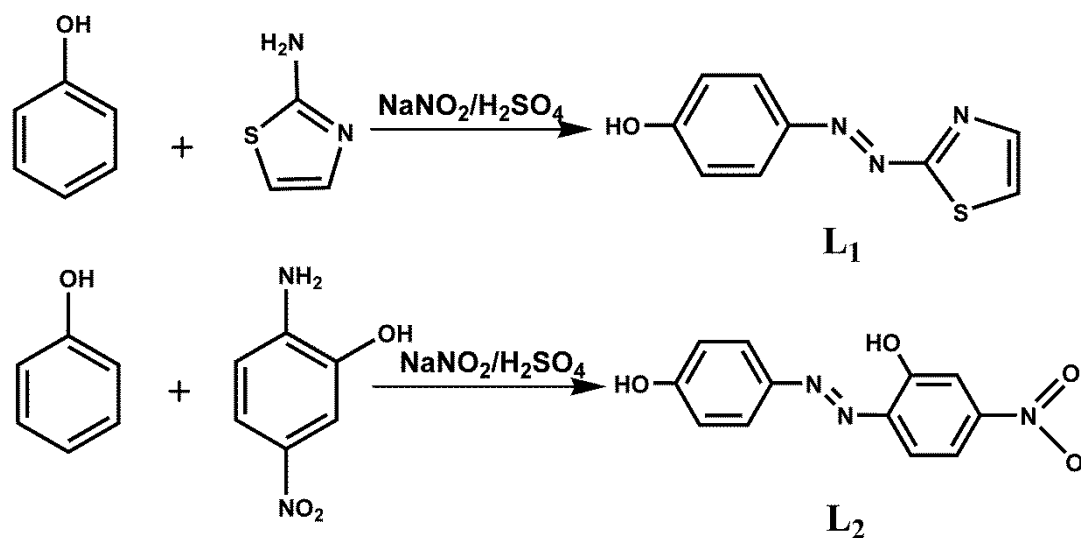
26. M. J. Peng, Y. Guo, X. F. Yang, L. Y. Wang and J. An, A highly selective ratiometric and colorimetric chemosensor for cyanide detection, *Dyes Pig.* 98 (2013) 327–332.
27. X. Sun, Y. Wang, X. Zhang, S. Zhang and Z. Zhang, A new coumarin based chromo-fluorogenic probe for selective recognition of cyanide ions in an aqueous medium, *RSC Adv.* 5 (2015) 96905–96910.
28. Y. Sun, Y. Liu and W. Guo, Fluorescent and chromogenic probes bearing salicylaldehyde hydrazone functionality for cyanide detection in aqueous solution, *Sens. Actuators B* 143 (2009) 171–176.
29. H. Huang, F. Chen, Z. Chen and M. Jiang, Synthesis and Z-scan measurements of third-order optical nonlinearity of azothiazole- and azobenzothiazole-containing side-chain polymers, *Polym. Bull.* 73 (2016) 1545–1552.
30. J. E. Huheey, E. A. Keiter and R. L. Keiter, *Inorganic chemistry: principles of structure and reactivity*, Harper Collins College Publishers, New York (1993).
31. M. Shortreed, R. Kopelman, M. Kuhn and B. Hoyland, Fluorescent fiber-optic calcium sensor for physiological measurements, *Anal. Chem.* 68 (1996) 1414–1418.
32. Y. Ding, T. Li, W. Zhu and Y. Xie, Highly selective colorimetric sensing of cyanide based on formation of dipyrin adducts, *Org. Biomol. Chem.* 10 (2012) 4201–4207.
33. V. Bhalla and R. M. Kumar, A pentaquinone based probe for relay recognition of F<sup>-</sup> and Cu<sup>2+</sup> ions: sequential logic operations at the molecular level, *Dalton Trans.* 42 (2013) 13390–13396.
34. M. J. Frisch, G. W. Trucks, H. B. Schlegel, G. E. Scuseria, M. A. Robb, J. R. Cheeseman, G. Scalmani, V. Barone, B. Mennucci, G. A. Petersson, H. Nakatsuji, M. Caricato, X. Li, H. P. Hratchian, A. F. Izmaylov, J. Bloino, G. Zheng, J. L. Sonnenberg, M. Hada, M. Ehara, K. Toyota, R. Fukuda, J. Hasegawa, M. Ishida, T. Nakajima, Y. Honda, O. Kitao, H. Nakai, T. Vreven, J. A. Montgomery Jr, J. E. Peralta, F. Ogliaro, M. Bearpark, J. J. Heyd, E. Brothers, K. N. Kudin, V. N. Staroverov, R. Kobayashi, J. Normand, K. Raghavachari, A. Rendell, J. C. Burant, S. S. Iyengar, J. Tomasi, M. Cossi, N. Rega, J. M. Millam, M. Klene, J. E. Knox, J. B. Cross, V. Bakken, C. Adamo, J. Jaramillo, R. Gomperts, R. E. Stratmann, O. Yazyev, A. J. Austin, R. Cammi, C. Pomelli, J. W. Ochterski, R. L. Martin, K. Morokuma, V. G. Zakrzewski, G. A. Voth, P. Salvador, J. J. Dannenberg, S. Dapprich, A. D. Daniels, O. Farkas, J. B. Foresman, J. V. Ortiz, J. Cioslowski, and D. J. Fox, *Gaussian 09, Revision A.02*, Gaussian, Inc., Wallingford CT, 2009.

35. M. S. Kumar and S. L. A. Kumar and A. Sreekanth, Highly selective fluorogenic anion chemosensors: naked-eye detection of  $F^-$  and  $AcO^-$  ions in natural water using a test strip, *Anal. Methods* 5 (2013) 6401–6410.

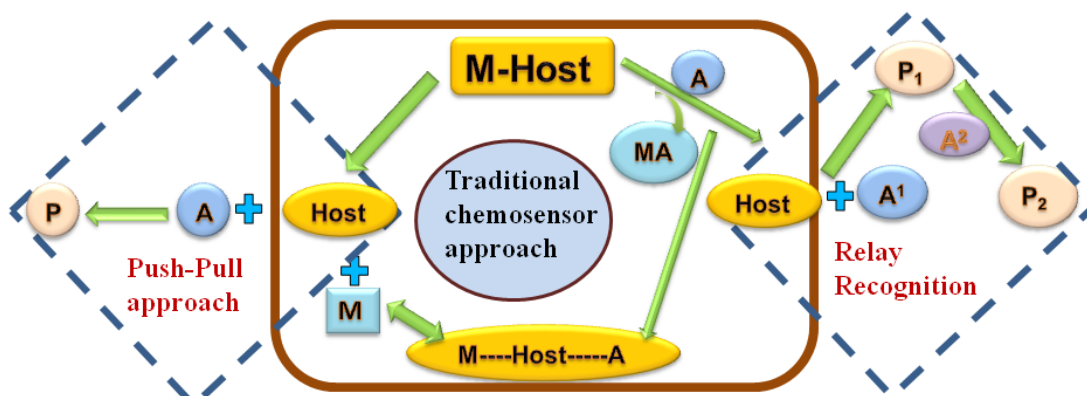
### Figure Captions

- Scheme 1.** Synthesis of 4-(thiazol-2-yl-diazenyl)phenol  $L_1$  and 2-((4-hydroxyphenyl)diazenyl)-5-nitrophenol  $L_2$ .
- Fig.1.** Illustration of “Anion Sensing”. A,  $A^1$ ,  $A^2$  = Anions, M=Metal, P,  $P_1$ ,  $P_2$ = Product, MA= ion pair.
- Fig.2.** Absorption spectra of  $L_1$  (20  $\mu$ M, DMSO/H<sub>2</sub>O-HEPES (v/v; 1:1, pH = 7.3 $\pm$ 0.2) solution) with a series of anions and sudden color change of  $L_1$  with CN<sup>-</sup> and AcO<sup>-</sup> ion, (b) Absorption spectra of  $L_2$  (20  $\mu$ M, DMSO/H<sub>2</sub>O-HEPES (v/v; 1:1, pH = 7.3 $\pm$ 0.2) solution) with a series of anions and Sudden color change of  $L_2$  with CN<sup>-</sup> and AcO<sup>-</sup> ion.
- Fig.3.** (a) Absorption spectra of  $L_1$  (20  $\mu$ M, DMSO/H<sub>2</sub>O-HEPES (v/v; 1:1, pH = 7.3 $\pm$ 0.2) solution) changes with increasing amount of CN<sup>-</sup> ion (0-100  $\mu$ L), Inset shows BH-plot of  $L_1$  with CN<sup>-</sup> ion, (b) Absorption spectra of  $L_1$  (20  $\mu$ M, DMSO/H<sub>2</sub>O-HEPES (v/v; 1:1, pH = 7.3 $\pm$ 0.2) solution) changes with increasing amount of AcO<sup>-</sup> ion (0-100  $\mu$ L), Inset shows BH-plot of  $L_1$  with AcO<sup>-</sup> ion.
- Fig.4.** (a) Absorption spectra of  $L_2$  (20  $\mu$ M, DMSO/H<sub>2</sub>O-HEPES (v/v; 1:1, pH = 7.3 $\pm$ 0.2) solution) changes with increasing amount of CN<sup>-</sup> ion (0-100  $\mu$ L), Inset shows BH-plot of  $L_2$  with CN<sup>-</sup> ion, (b) Absorption spectra of  $L_2$  (20  $\mu$ M, DMSO/H<sub>2</sub>O-HEPES (v/v; 1:1, pH = 7.3 $\pm$ 0.2) solution) changes with increasing amount of AcO<sup>-</sup> ion (0-100  $\mu$ L), Inset shows BH-plot of  $L_2$  with AcO<sup>-</sup> ion.
- Fig.5.** (a) Interference study of different anions with the selectivity of  $L_1$  towards CN<sup>-</sup> ion (b) Interference study of different anions with the selectivity of  $L_2$  towards CN<sup>-</sup> ion.
- Fig.6.** <sup>1</sup>H-NMR titration of  $L_1$  with CN<sup>-</sup> ion in DMSO-*d*<sub>6</sub>.
- Fig.7.** <sup>1</sup>H-NMR titration of  $L_2$  with CN<sup>-</sup> ion in DMSO-*d*<sub>6</sub>.
- Fig.8.** Optimized structure of  $L_1$  and  $L_2$  and their cyanide adduct.
- Fig.9.** HOMO-LUMO energy diagram of  $L_1$ ,  $L_1$ +CN<sup>-</sup>,  $L_2$  and  $L_2$ +CN<sup>-</sup>.
- Fig.10.** Photographs of test strips of  $L_1$  and  $L_2$  with CN<sup>-</sup> and AcO<sup>-</sup> ion.
- Fig.11.** (a) Absorbance changes at 485 nm for  $L_1$  (20  $\mu$ M, 25 $^\circ$ C) in a mixture of DMSO-H<sub>2</sub>O (1:1, v/v) after addition of NaCN (1mM) (b) Absorbance

changes at 432 nm for  $L_2$  (20  $\mu$ M, 25 $^\circ$ C) in a mixture of DMSO–H<sub>2</sub>O (1:1, v/v) after addition of NaCN (1mM).



Scheme 1. Synthesis of 4-(thiazol-2-yl)diazenylphenol  $L_1$  and 2-((4-hydroxyphenyl)diazenyl)-5-nitrophenol  $L_2$ .



v

Fig.1. Illustration of "Anion Sensing". A, A<sup>1</sup>, A<sup>2</sup> = Anions, M=Metal, P, P<sub>1</sub>, P<sub>2</sub>= Product, MA= ion pair.

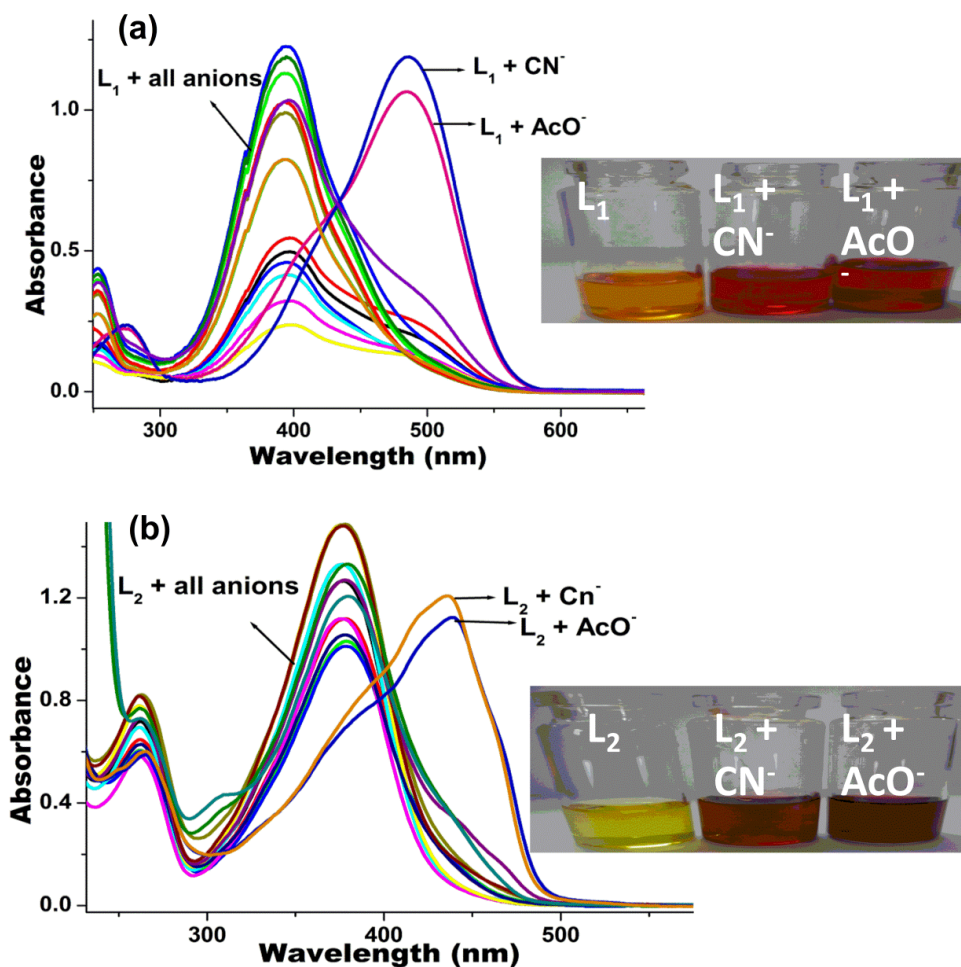


**Fig.2.** (a) Absorption spectra of  $L_1$  (20  $\mu\text{M}$ , DMSO/ $\text{H}_2\text{O}$ -HEPES (v/v; 1:1, pH =  $7.3 \pm 0.2$ ) solution) with a series of anions and sudden color change of  $L_1$  with  $\text{CN}^-$  and  $\text{AcO}^-$  ion, (b) Absorption spectra of  $L_2$  (20  $\mu\text{M}$ , DMSO/ $\text{H}_2\text{O}$ -HEPES (v/v; 1:1, pH =  $7.3 \pm 0.2$ ) solution) with a series of anions and sudden color change of  $L_2$  with  $\text{CN}^-$  and  $\text{AcO}^-$  ion.

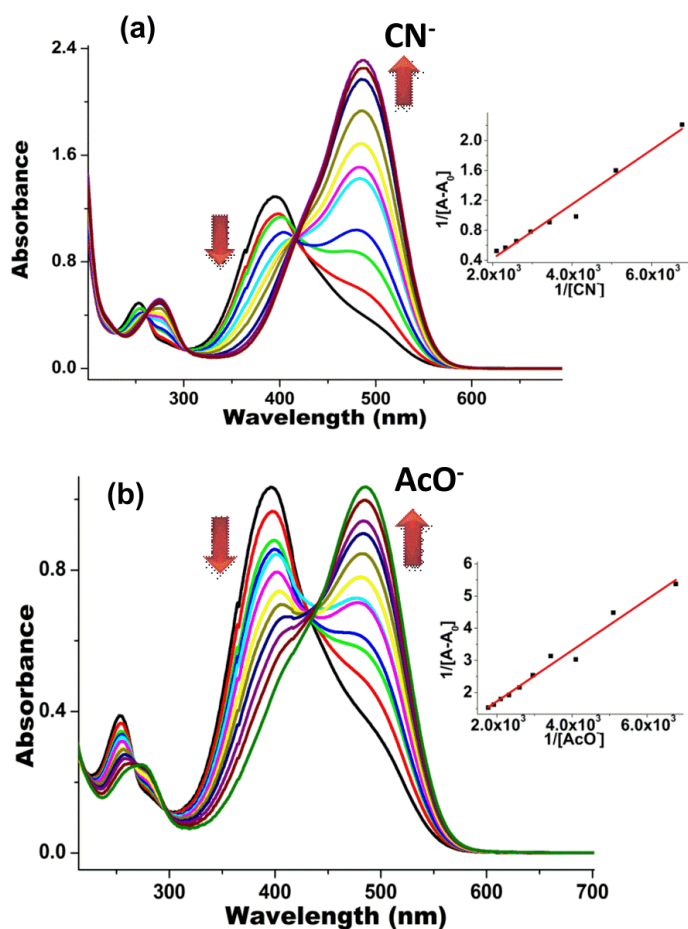


**Fig.3.** (a) Absorption spectra of  $L_1$  (20  $\mu\text{M}$ , DMSO/ $\text{H}_2\text{O}$ -HEPES (v/v; 1:1, pH =  $7.3 \pm 0.2$ ) solution) changes with increasing amount of  $\text{CN}^-$  ion (0-100  $\mu\text{L}$ ), Inset shows BH-plot of  $L_1$  with  $\text{CN}^-$  ion, (b) Absorption spectra of  $L_1$  (20  $\mu\text{M}$ , DMSO/ $\text{H}_2\text{O}$ -HEPES (v/v; 1:1, pH =  $7.3 \pm 0.2$ ) solution) changes with increasing amount of  $\text{AcO}^-$  ion (0-100  $\mu\text{L}$ ), Inset shows BH-plot of  $L_1$  with  $\text{AcO}^-$  ion.

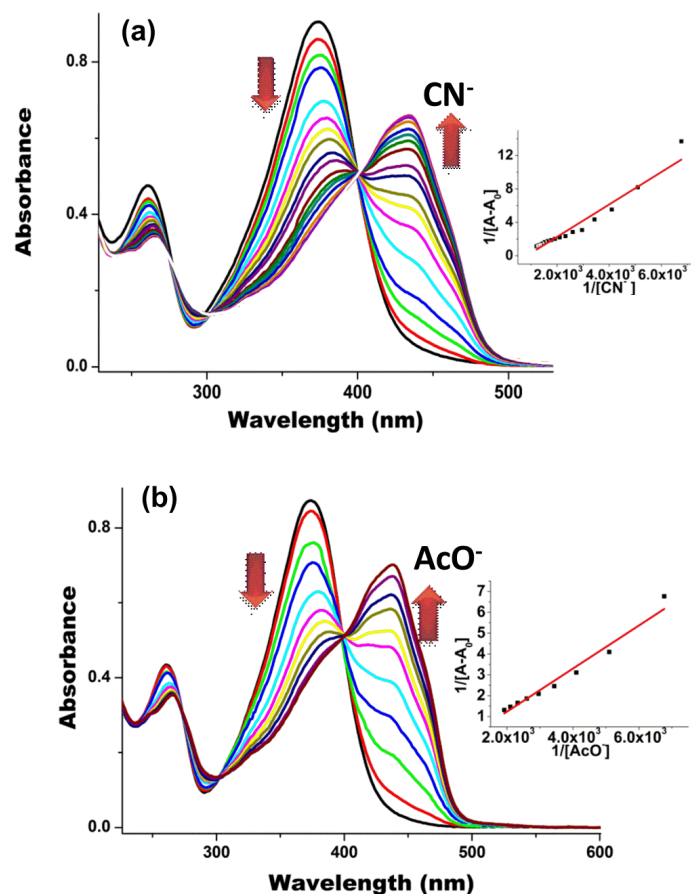


**Fig.4.** (a) Absorption spectra of L<sub>2</sub> (20 μM, DMSO/H<sub>2</sub>O-HEPES (v/v; 1:1, pH = 7.3±0.2) solution) changes with increasing amount of CN<sup>-</sup> ion (0-100 μL), Inset shows BH-plot of L<sub>2</sub> with CN<sup>-</sup> ion, (b) Absorption spectra of L<sub>2</sub> (20 μM, DMSO/H<sub>2</sub>O-HEPES (v/v; 1:1, pH = 7.3±0.2) solution) changes with increasing amount of AcO<sup>-</sup> ion (0-100 μL), Inset shows BH-plot of L<sub>2</sub> with AcO<sup>-</sup> ion.

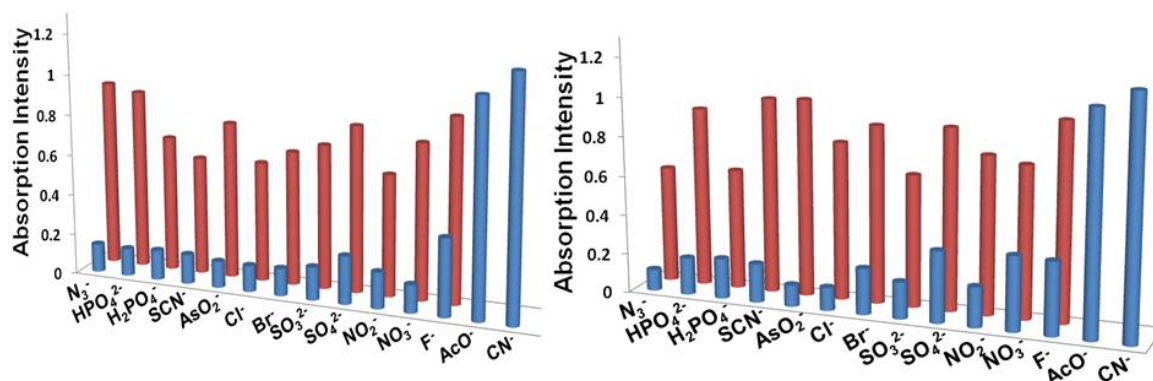


**Fig.5.** (a) Interference study of different anions with the selectivity of L<sub>1</sub> towards CN<sup>-</sup> ion (b) Interference study of different anions with the selectivity of L<sub>2</sub> towards CN<sup>-</sup> ion.

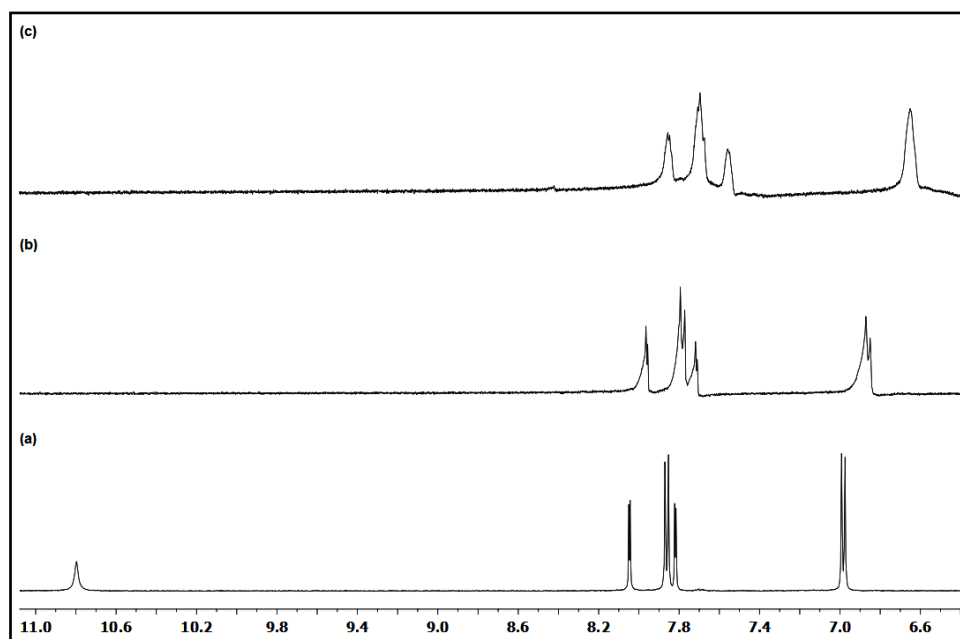


Fig.6.  $^1\text{H-NMR}$  titration of  $\text{L}_1$  with  $\text{CN}^-$  ion in  $\text{DMSO-}d_6$ .

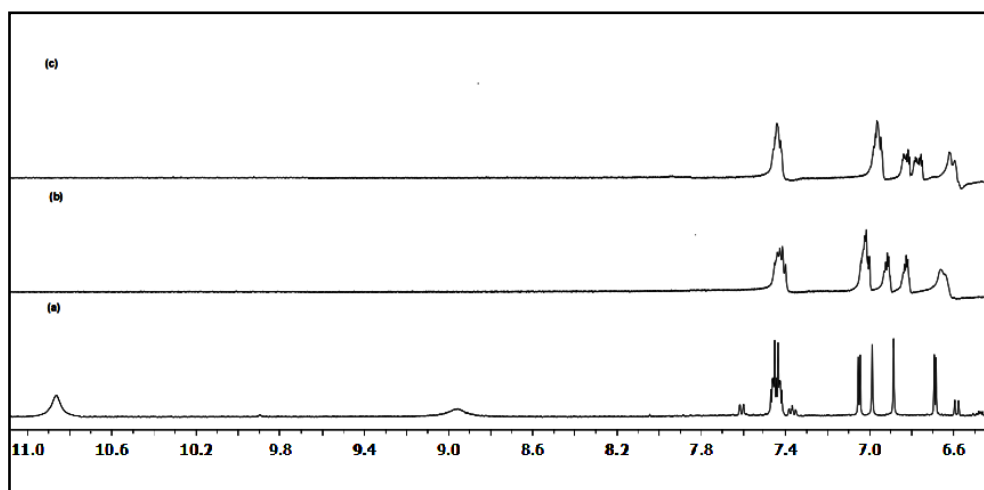


Fig.7.  $^1\text{H-NMR}$  titration of  $\text{L}_2$  with  $\text{CN}^-$  ion in  $\text{DMSO-}d_6$ .

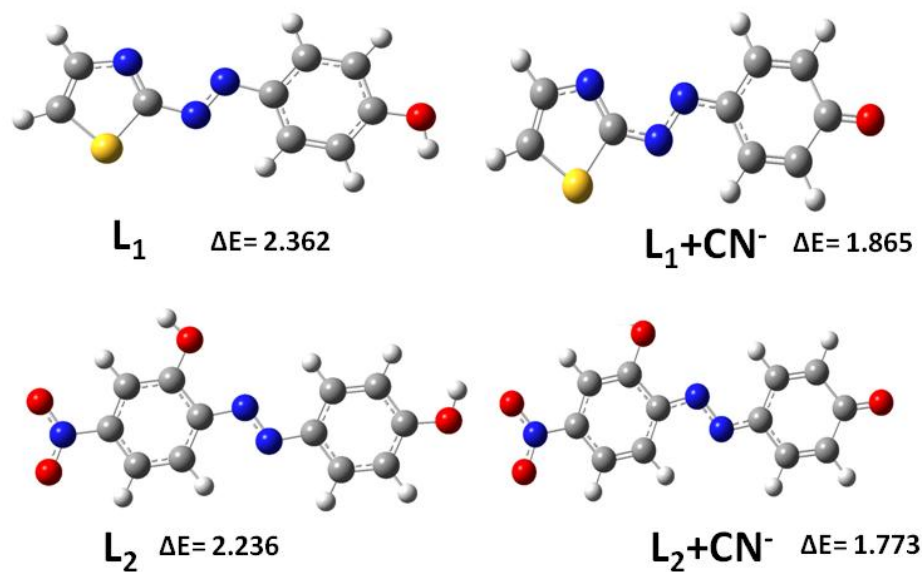


Fig.8. Optimized structure of  $L_1$  and  $L_2$  and their cyanide adduct.

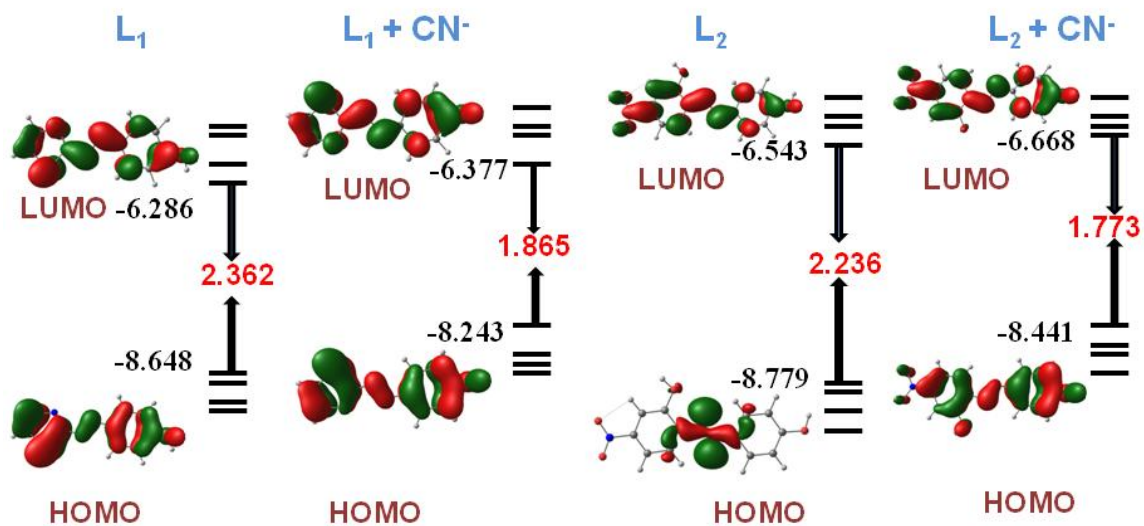
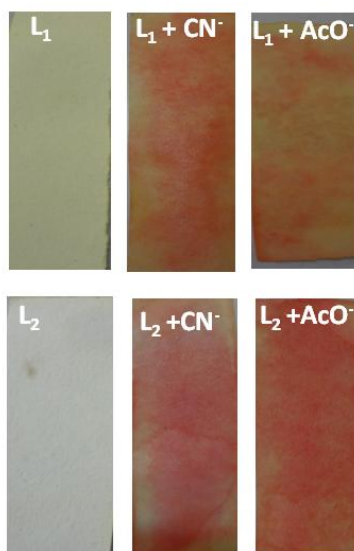
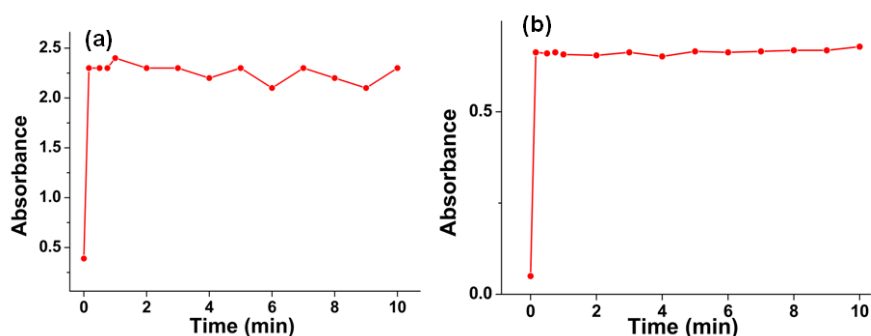


Fig.9. HOMO-LUMO energy diagram of  $L_1$ ,  $L_1+CN^-$ ,  $L_2$  and  $L_2+CN^-$ .



**Fig.10.** Photographs of test strips of L<sub>1</sub> and L<sub>2</sub> with CN<sup>-</sup> and AcO<sup>-</sup> ion.



**Fig.11.** (a) Absorbance changes at 485 nm for L<sub>1</sub> (20 μM, 25°C) in a mixture of DMSO–H<sub>2</sub>O (1:1, v/v) after addition of NaCN (1mM) (b) Absorbance changes at 432 nm for L<sub>2</sub> (20 μM, 25°C) in a mixture of DMSO–H<sub>2</sub>O (1:1, v/v) after addition of NaCN (1mM).

### Tables

**Table 1.** Stoichiometry, binding constant, detection limit values for obtained adduct of L<sub>1</sub> and L<sub>2</sub> with CN<sup>-</sup> and AcO<sup>-</sup> ions.

S. No.	Receptor + ions	Solvent	Binding Constant	Stoichiometry	Limit of Detection (nM)
1.	L <sub>1</sub> + CN <sup>-</sup>	DMSO/H <sub>2</sub> O (1:1)	$1.6 \times 10^3$	1:1	87
2.	L <sub>1</sub> + AcO <sup>-</sup>	DMSO/H <sub>2</sub> O (1:1)	$8.0 \times 10^2$	1:1	83
3.	L <sub>2</sub> + CN <sup>-</sup>	DMSO/H <sub>2</sub> O (1:1)	$8.4 \times 10^3$	1:2	81
4.	L <sub>2</sub> + AcO <sup>-</sup>	DMSO/H <sub>2</sub> O (1:1)	$1.7 \times 10^2$	1:2	89

**Table 2. Energy of HOMO-LUMO of L<sub>1</sub>, L<sub>2</sub> and Complexes.**

Receptor + ions	HOMO (eV)	LUMO (eV)	$\Delta E$ (eV)
L <sub>1</sub>	-8.648	-6.286	2.362
L <sub>1</sub> + CN <sup>-</sup>	-8.243	-6.377	1.865
L <sub>2</sub>	-8.779	-6.543	2.236
L <sub>2</sub> + CN <sup>-</sup>	-8.441	-6.68	1.773